J Paleolimnol (2014) 52:27–41
DOI 10.1007/s10933-014-9776-4

ORIGINAL PAPER

Sclerochronological oxygen and carbon isotope ratios in *Radix* (Gastropoda) shells indicate changes of glacial meltwater flux and temperature since 4,200 cal yr BP at Lake Karakul, eastern Pamirs (Tajikistan)

Linda Taft · Steffen Mischke · Uwe Wiechert · Christian Leipe · Ilhomjon Rajabov · Frank Riedel

Received: 13 June 2013 / Accepted: 28 March 2014 / Published online: 20 April 2014

Abstract We report $\delta^{18}O$ and $\delta^{13}C$ values of 21 fossil shells from the aquatic gastropod *Radix* from a sediment core taken in the eastern basin of Lake Karakul, Tajikistan (38.86–39.16°N, 73.26–73.56°E, 3,928 m above sea level) and covering the last 4,200 cal yr BP. The lake is surrounded by many palaeoshorelines evidencing former lake-level changes, most likely triggered by changes in meltwater flux. This hypothesis was tested by interpreting the isotope ratios of *Radix* shells together with $\delta^{18}O$ values of Ostracoda and of authigenic aragonite. The mean $\delta^{18}O$ values of *Radix* and Ostracoda fall along the same long-term trend indicating a change in the isotopic composition of precipitation, which contributed to the glaciers in the catchment as snow and finally as melt water to the lake. The sclerochronological $\delta^{18}O$ and $\delta^{13}C$ patterns in *Radix* shells provide seasonal weather information, which is discussed in context with previously proposed climatic changes during the last 4,200 cal yr BP. The period between ~4,200 and 3,000 cal yr BP was characterized by stepwise glacier advance in the catchment most likely due to a precipitation surplus. Subsequently the climate remained relatively cold but the lake level fluctuated, as indicated by ostracod shell isotope data. From ~1,800 cal yr BP the sclerochronological

L. Taft (✉) · S. Mischke · U. Wiechert · C. Leipe · F. Riedel
Institute of Geological Sciences, Free University Berlin, Malteserstr. 74-100, 12249 Berlin, Germany
e-mail: linda.taft@fu-berlin.de

S. Mischke
e-mail: smischke@geo.uni-potsdam.de

U. Wiechert
e-mail: wiechert@zedat.fu-berlin.de

C. Leipe
e-mail: c.leipe@fu-berlin.de

F. Riedel
e-mail: paleobio@zedat.fu-berlin.de

S. Mischke
Institute of Earth and Environmental Science, University of Potsdam, Karl-Liebknecht-Str. 24-25, 14476 Potsdam, Germany

I. Rajabov
State Administration for Hydrometeorology of the Committee for Environmental Protection Under the Government of the Republic of Tajikistan, 47 Shevchenko Str., Dushanbe 734025, Tajikistan
e-mail: ilhomrajabov@mail.ru

F. Riedel
Key Laboratory of Plateau Lake Ecology and Global Change, College of Tourism and Geography, Yunnan Normal University, No. 1 Yuhua District, Chenggong, Kunming 650500, China

patterns provide evidence for increasing melt water flux and transport of allochthonous carbon into the lake, most likely due to an accelerated glacier retreat. The period around 1,500 cal yr BP was characterized by strong warming, increasing meltwater flux, glacier retreat and an increasing lake level. Warm conditions continued until ~500 cal yr BP probably representing the end of the Medieval Warm Period. A short relatively cold (dry?) period and a lower lake level are assumed for ~350 cal yr BP, possibly an analogue to the Maunder Minimum cooling in the North Atlantic region. Our results show that the lake system is complex, and that changes were triggered by external forcing and feedbacks. The similarity of $\delta^{18}O$ values in *Radix* and ostracod shells demonstrates that both archives provide complementary information.

Keywords Palaeolimnology · Stable isotopes · Gastropods · Sclerochronology · Late Holocene · Central Asia

Introduction

The dynamics of mountain glaciers are among the most visible indications of the effects of climatic changes (Solomina et al. 2004; IPCC Report 2007), and it has been observed that many glaciers all over the world melted in response to warmer air temperatures during the last 150 years (World Glacier Monitoring Service 2012). However, timing and extent of glacial responses are highly variable and depend on size, location and climate regime (Bolch 2007). In most areas of Central Asia, the glaciers retreated since the termination of the Little Ice Age (LIA; Solomina et al. 2004; Khromova et al. 2006; Bolch 2007; Kutuzov and Shahgedanova 2009). On the other hand, more than 50 % of observed glaciers in the Karakoram region are advancing or have remained stable during the last decade (Scherler et al. 2011). As long as glaciers are large, one visible response of glacial retreat is meltwater discharge, which can cause rising water levels in glacier-fed lakes (Sorrel et al. 2006; Komatsu et al. 2010; Osipov and Khlystov 2010). Glacier and meltwater fluctuations in modern and historical times can be monitored by remote sensing, morphologic and mass-balance studies, or can be evaluated from written records (Solomina et al. 2004; Khromova et al. 2006; Narama et al. 2010). Variations that occurred further back in time can only be modeled (Sarikaya et al. 2009; Goehring et al. 2012) or reconstructed from proxy data indicating glacier stages, temperature fluctuations or freshwater supply (Ricketts et al. 2001; Owen et al. 2002; Seong et al. 2007, 2009). Lakes represent important systems in this context because they archive a number of suitable proxies in their sediments (Wünnemann et al. 2006; Mischke and Zhang 2010; Vasskog et al. 2012).

Of special interest are lakes located in regions that are particularly sensitive to environmental and climatic changes. One example is Lake Karakul, located in the eastern Pamir Mountains of Tajikistan (Fig. 1). Palaeoshorelines up to 205 m above the modern lake level provide evidence for lake dynamics that were related to Pleistocene climate fluctuations (Komatsu 2009; Komatsu et al. 2010). Mischke et al. (2010) analyzed a 104-cm-long sediment core, covering the last 4,200 cal yr BP, studying geochemical, granulometrical and palynological properties and concluded that the data indicate mainly air temperature-driven changes in meltwater supply due to the presence of glaciers in the catchment area and the aridity of the region. However, the qualitative characterization of meltwater supply and other processes that influence lake level changes could not be provided.

$\delta^{18}O$ and $\delta^{13}C$ signals from fossil ostracod shells have been used for the palaeolimnological reconstruction (Mischke et al. 2010). As ostracods shed and build their valves several times during ontogeny, sclerochronological analyses that could cover the annual hydrological cycle from which the meltwater signal can be inferred are not practical. Mischke et al. (2010) interpreted the ostracod isotope data with qualification because palaeoecological inferences did not appear to be indicated by the studied taxon, which is probably endemic.

Taft et al. (2012, 2013) have demonstrated that sclerochronological $\delta^{18}O$ and $\delta^{13}C$ patterns in aragonite shells of the aquatic gastropod *Radix* mirror seasonal variations in modern lakes across the Tibetan Plateau. Ice cover duration, meltwater discharge, precipitation and evaporation periods can be differentiated. The method also has been applied to modern shells of Lake Karakul (Taft et al. 2013).

In the here presented study, we adopt the method to fossil *Radix* shells from late Holocene sediments of Lake Karakul and evaluate whether late Holocene

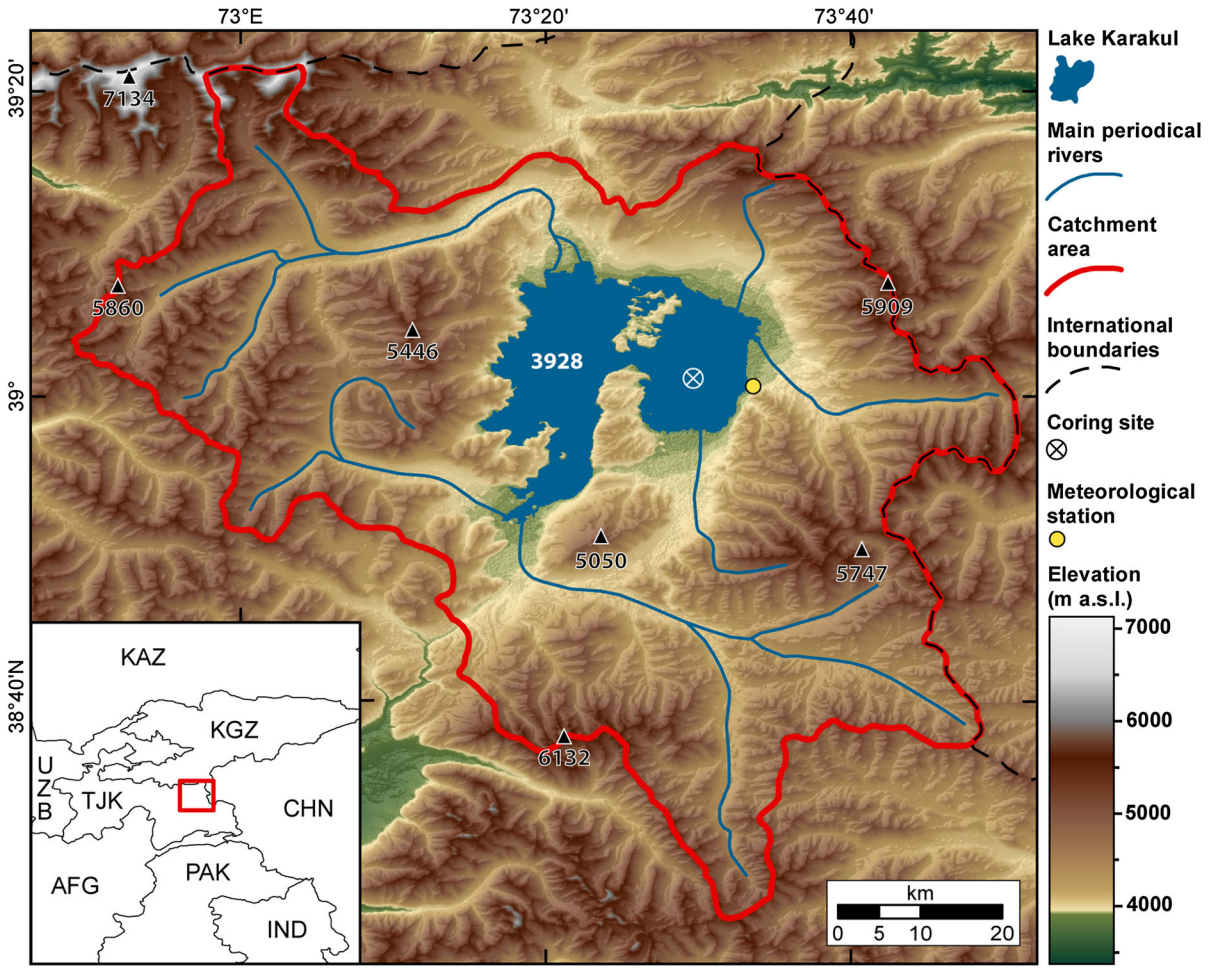

Fig. 1 Lake Karakul with core location and periodical inflows. The catchment area of Lake Karakul spans 4,464 km^2

meltwater input rates can be inferred from the shells, and can be related to temperature changes and glacier fluctuations in the catchment. We further consider whether the shell data can be related to the geochemical results of Mischke et al. (2010) to improve our understanding about the hydrological system.

Study area

Karakul (38.86–39.16°N, 73.26–73.56°E, 3,928 m above sea level) is an endorheic mesohaline lake in the eastern Pamirs in Tajikistan, (Fig. 1) which are part of the extensive high mountain system of Central Asia, comprising the Pamir-Karakoram-Hindu-Kush ranges. The lake consists of a relatively shallow eastern sub-basin with a maximum water depth of approximately 20 m and a deep western sub-basin with a water depth of 242 m (Molchanov 1929). The catchment area spans 4,464 km^2. The surface area of the lake is about 380 km^2 (Komatsu et al. 2010), and is covered by ice of up to about 1 m thick from the end of November until the end of May (Mischke et al. 2010). The lake is located in a tectonic graben basin (Melack 1983; Hammer 1986; Gopal and Ghosh 2010), but an origin as a meteor-impact structure also was discussed in the past (Gurov et al. 1993; Safarov 2006). The highest mountain peak in the catchment area is above 6,000 m asl. Many of the surrounding mountains are covered by snow and ice, which are the most important sources of the lake water (Ni et al. 2004). The main seasonally active inflow is located at the northern shore of the lake (Fig. 1).

Three water samples from the eastern basin have $\delta^{18}O$ values ranging from −3.8 to −3.5 ‰ relative to

V-SMOW. Inflowing streams, which transport predominantly glacial meltwater, have values ranging from −18.0 to −14.0 ‰ (Mischke et al. 2010). The comparatively high $\delta^{18}O$ value of the lake water mirrors the long residence time and the strong influence of insolation, which results in low air humidity and high evaporation from the lake surface.

Lake Karakul is located in an area dominated by the Westerly wind system. Because the high mountain ranges to the west block the Westerly moisture penetration into the lake catchment (Komatsu et al. 2010), the annual precipitation is only 82 mm, with slightly higher precipitation between March and July and least precipitation during the winter months (Mischke et al. 2010). With a mean annual temperature of about −4 °C, the climate is characterized as cold semi-arid BSk in the Köppen-Geiger climate classification (Peel et al. 2007).

Komatsu (2009) and Komatsu et al. (2010) studied the palaeoshorelines and reconstructed a lake history for the Mid- to Late Pleistocene based on remote sensing data, field mapping and tentative chronology. They classified four groups of shorelines that indicated higher or constant lake levels, which were correlated to the glacial maxima of MIS 8, 6, 4 and 2. Geomorphic glacial landforms showed that Pleistocene glaciers came close to the modern eastern, northern and southern lake shore (Komatsu et al. 2010; Mischke et al. 2010). Nothing is known about the Holocene glacial history of the Lake Karakul region and only a few data exist for modern times. On the base of dendrochronological data, colder conditions were concluded for 1897–1916 indicating a glacier advance in the drainage area of Lake Karakul (Ni et al. 2004). For 1925–1980, it is assumed that the glacier area in the lake catchment decreased (Ni et al. 2004), probably in response to global warming. Based on historical surveys and remote sensing, Khromova et al. (2006) detected a glacier decrease between 1978–2001 in the eastern Pamir region. However, detailed glacial studies in the catchment of Lake Karakul have not been conducted yet.

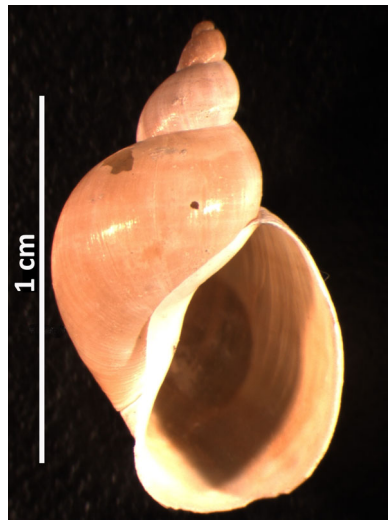

Fig. 2 Example of a well-preserved fossil *Radix* shell from Lake Karakul

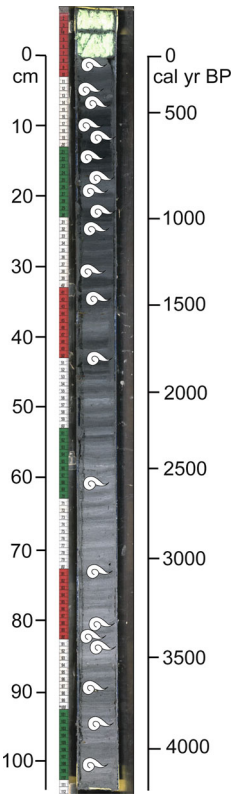

Fig. 3 Sediment core of 104 cm length taken from the eastern sub-basin of Lake Karakul (Mischke et al. 2010) with positions of fossil *Radix* shells

Materials and methods

The catchment area of Lake Karakul was calculated in ArcGIS v10.0 (ESRI 2011) with the use of HydroSHEDS v1.0 data (Lehner and Döll 2004; Lehner et al. 2006) in the projected coordinate reference system Pulkovo 1942/3-degree Gauss-Kruger CM 72E (EPSG: 2599).

Shell sampling and preparation

Twenty-one *Radix* (Fig. 2) shells (17 complete shells and four large fragments) were collected from 21 sediment layers from a core of 104 cm length (Fig. 3). The core was obtained from 19.1 m water depth in the center of the eastern sub-basin of Lake Karakul (Fig. 1), and it covers the last 4,200 cal yr BP (Mischke et al. 2010). Modern *Radix* specimens from Lake Karakul represent the species *Radix auricularia* (Linnaeus 1758) (von Oheimb et al. 2011). Fossil shells from the core showed the same shell morphology and thus were assigned to the same species. Details about biology, shell growth, life cycle, nutrition, etc. are presented in Taft et al. (2012, 2013).

The shells were cleaned manually and in an ultrasonic bath and subsequently treated with H_2O_2 for 24 h to remove remaining organic matter before they were dried for 24 h at room temperature. The shells were sampled for stable isotope analysis in a constant distance of 1 mm along the ontogenetic spiral of growth increments using a dental drill. Depending on shell size and total number of whorls, we obtained 7–25 sub-samples per shell. The sub-samples were labeled in alphabetical order beginning with [a], which represents the latest shell part. The four shell fragments (from core layers 10; 30; 61 and 101 cm) were homogenized and isotopically analyzed as powdered bulk samples.

Stable isotope analysis

The aragonite shell samples were isotopically analyzed at the Freie Universität Berlin using a GasBench II linked to a MAT-253 ThermoFisher Scientific™ isotope ratio mass spectrometer. The external error of the measurements is ±0.06 ‰ for $\delta^{18}O$ and ±0.04 ‰ for $\delta^{13}C$ both 1 SD (standard deviations) based on the reproducibility of the in-house reference material Laaser marble. The measurements were standardized against Carrara Marble (CAM) and Kaiserstuhl carbonatite in-house reference material (KKS) which had been calibrated against Vienna PeeDee Belemnite (V-PDB) international isotope reference material using NBS-18 and NBS-19. All results are reported in δ notation relative to V-PDB (Table 1; Figs. 4, 5c, d). Average isotope values are the arithmetic mean values of all sub-samples per shell.

Results

Average $\delta^{18}O$ and $\delta^{13}C$ shell values

Average $\delta^{18}O$ shell values cover a range from −1.4 to 0.9 ‰. The highest values occur at 95 cm (0.9 ‰), 83 cm (0.2 ‰) and 15 cm (0.4 ‰) core depth (Table 1; Fig. 5c). The values are low at 43 cm (−1.1 ‰) and from 6 cm core depth to the top (from −1.4 to −0.9 ‰). From the deepest part of the core to the top, a trend to more negative values is visible (Fig. 5c). This general trend is interrupted by excursions to more positive values (at 95, 83, 61, 35, 30, 15 and 10 cm core depth). The shifts at 95 cm (0.9 ‰), 83 cm (0.2 ‰) and 15 cm (0.4 ‰) core depth are most pronounced.

Average $\delta^{13}C$ shell values cover a range from −1.5 to 1.7 ‰. The highest values occur at 81 cm (1.5 ‰), 30 cm (1.1 ‰) and 10 cm (1.7 ‰) core depth (Table 1). The values are relatively low at 83 cm (−1.0 ‰), 25 cm (−1.5 ‰) and 1 cm (−0.9 ‰) core depth.

Sclerochronological $\delta^{18}O$ and $\delta^{13}C$ variations

$\delta^{18}O$ intra-shell values of all samples cover a range from −2.1 to 1.4 ‰. $\delta^{13}C$ values are in a range from −3.3 to 2.6 ‰. The isotope values for each sub-sample are presented in Table 1 and the sclerochronological patterns are shown in Fig. 4.

Sub-samples from 73 and 43 cm core depth exhibit the highest $\delta^{18}O$ variability (>1.6 ‰) of all samples. Sub-samples from 89 and 6 cm core depth feature the lowest variability (<0.6 ‰). Sub-samples from 83 and 25 cm core depth show the highest $\delta^{13}C$ variability (4.4 and 3.5 ‰) and sub-sample from 15 cm core depth exhibits the lowest variability (0.4 ‰).

Discussion

What do gastropod, ostracod and authigenic carbonates record?

In a multi-proxy study, Mischke et al. (2010) concluded that the Ostracoda taxon from Lake Karakul is probably not suitable for palaeoecological inferences and discussed solely authigenic carbonates. However,

Table 1 Individial mean and absolute $\delta^{18}O$ and $\delta^{13}C$ values for each shell sub-sample

Core depths cm	1		5		6		10		11		15		18		19		23		25	
Sub-samples	$\delta^{18}O$	$\delta^{13}C$	$\delta^{18}O$	$\delta^{13}C$	$\delta^{18}O$	$\delta^{13}C$	$\delta^{18}O$	$\delta^{13}C$	$\delta^{18}O$	$\delta^{13}C$	$\delta^{18}O$	$\delta^{13}C$	$\delta^{18}O$	$\delta^{13}C$	$\delta^{18}O$	$\delta^{13}C$	$\delta^{18}O$	$\delta^{13}C$	$\delta^{18}O$	$\delta^{13}C$
Ø	−0.18	−0.87	−1.37	−0.36	−1.43	0.70	−0.30	1.70	−0.76	0.96	0.36	0.62	−0.75	−0.25	−0.77	0.71	−0.31	0.57	−0.64	−1.53
a	**−0.18**	**0.37**	−0.97	−0.77	−1.56	0.91			**−0.15**	**0.00**	0.26	**0.82**	−0.94	0.32	**−0.21**	**1.22**	**0.11**	0.89	**0.00**	**0.21**
b	−0.55	−0.84	−1.68	−0.69	−1.20	**1.07**			−0.16	1.00	**0.84**	0.56	−0.73	0.07	−0.22	1.07	−0.27	0.68	−0.54	−0.29
c	−0.26	−0.38	−1.68	0.44	−1.45	1.03			−0.40	1.01	0.41	**0.45**	−1.01	−0.60	−0.91	0.73	−0.42	0.76	−0.65	−0.31
d	−0.86	−0.69	−1.79	0.15	**−1.63**	0.62			−0.54	1.13	**−0.09**	0.53	−0.62	0.24	−0.93	**0.41**	**−0.70**	0.66	−0.66	−0.27
e	−1.07	−0.65	**−1.87**	**0.44**	**−1.17**	0.60			−0.29	0.74	0.15	0.56	−0.68	0.59	−0.96	0.56	−0.69	0.78	−0.28	−0.17
f	−1.23	−0.17	−1.51	0.31	−1.58	**−0.02**			**−1.30**	1.07	0.31	0.73	−0.53	0.64	−0.95	0.75	−0.43	0.87	−0.26	0.09
g	−0.99	−0.26	−1.74	−0.01					−1.25	1.05	0.61	0.71	−0.49	0.55	−0.83	0.62	−0.40	0.65	−0.42	−0.85
h	−1.16	−0.29	−1.22	−0.02					−1.20	0.68			−0.34	0.50	−0.93	0.54	−0.25	**1.07**	−0.75	−1.75
i	−1.11	−1.36	−1.28	−0.32					−0.84	0.57			−0.69	**0.91**	−0.58	1.15	−0.20	0.57	−0.97	−2.19
j	−0.89	−1.49	−1.18	−0.29					−0.77	1.40			−1.02	−0.23	−0.35	0.80	−0.46	0.13	−1.07	−2.81
k	−0.28	0.22	−1.16	−0.32					−0.90	1.31			−1.05	−0.97	−0.45	0.51	−0.44	**−0.04**	−1.01	−2.29
l	−1.05	−0.52	**−0.71**	0.05					−1.14	1.07			−1.03	−0.88	−0.69	0.61	−0.16	0.39	**−1.15**	−3.17
m	−1.19	−2.18	−1.54	−0.79					−1.15	1.05			−0.73	0.47	−0.92	0.50	0,10	−0.02	−0.83	−1.78
n	−1.17	−0.25	−1.47	−0.40					−0.83	0.90			**−1.06**	**−1.23**	**−1.18**	0.49	−0.42	0.61	−0.94	**−3.29**
o	−1.24	**−2.41**	n.d.	n.d.					−0.43	**1.45**			−0.72	−1.12	−0.98	0.86	−0.08	0.58	−0.93	−2.88
p	−1.29	−2.33	−1.44	−0.89									**−0.29**	−1.05	−1.16	0.60			−0.71	−2.20
q	−0.81	−0.84	−1.40	**−1.09**									−0.88	−0.87					−0.60	−1.62
r	−1.09	−1.55	−1.22	−0.81									−0.70	−1.16					−0.96	−2.21
s	**−1.29**	−0.99	−1.06	−0.73									−0.68	−1.02					−0.73	−2.15
t			−1.14	−0.60															−0.75	−2.47
u			−1.27	−0.38															−0.13	−1.36
v			−1.38	−0.76															−0.21	−1.00
w																			−0.28	−0.51
x																				
y																				

Core depths cm	30		35		43		61		73		81		83		84		89		95		101	
Sub-samples	$\delta^{18}O$	$\delta^{13}C$	$\delta^{18}O$	$\delta^{13}C$	$\delta^{18}O$	$\delta^{13}C$	$\delta^{18}O$	$\delta^{13}C$	$\delta^{18}O$	$\delta^{13}C$	$\delta^{18}O$	$\delta^{13}C$	$\delta^{18}O$	$\delta^{13}C$	$\delta^{18}O$	$\delta^{13}C$	$\delta^{18}O$	$\delta^{13}C$	$\delta^{18}O$	$\delta^{13}C$	$\delta^{18}O$	$\delta^{13}C$
Ø	−0.04	1.11	−0.13	−0.04	−0.96	−0.26	−0.28	0.67	−0.75	−0.33	−0.55	1.53	0.23	−1.18	−0.39	0.63	−0.19	−0.47	0.86	0.70	−0.49	0.59
a			0.36	0.01	**−0.13**	**0.73**			**−0.03**	0.27	**−0.85**	1.09	n.d.	n.d.	**0.20**	0.90	−0.27	−0.09	0.82	0.56		
b			−0.01	−0.12	1.37	0.07			−0.67	**0.69**	−0.82	1.86	0.50	1.03	0.17	0.96	−0.18	−0.18	0.99	0.56		
c			−0.45	−0.35	−0.95	0.16			**−2.01**	**−1.38**	−0.82	**0.57**	0.52	**1.30**	−0.22	0.95	**−0.56**	−0.46	**1.42**	1.08		
d			−0.46	−0.13	−0.34	−0.11			−0.84	−0.66	−0.71	1.56	0.30	−0.79	**−0.82**	**1.03**	−0.01	0.03	0.98	0.71		
e			−0.25	0.05	−0.60	−0.09			−0.78	−0.20	**−0.04**	1.21	0.74	0.81	−0.73	0.88	−0.19	**0.21**	0.62	0.76		

Table 1 continued

Core depths cm	30		35		43		61		73		81		83		84		89		95		101	
Sub-samples	$\delta^{18}O$	$\delta^{13}C$	$\delta^{18}O$	$\delta^{13}C$	$\delta^{18}O$	$\delta^{13}C$	$\delta^{18}O$	$\delta^{13}C$	$\delta^{18}O$	$\delta^{13}C$	$\delta^{18}O$	$\delta^{13}C$	$\delta^{18}O$	$\delta^{13}C$	$\delta^{18}O$	$\delta^{13}C$	$\delta^{18}O$	$\delta^{13}C$	$\delta^{18}O$	$\delta^{13}C$	$\delta^{18}O$	$\delta^{13}C$
f			−0.31	−0.03	−0.64	−0.35			−0.82	−0.84	−0.82	**2.61**	0.52	−0.19	−0.40	0.90	−0.19	0.10	**0.52**	1.01		
g			−0.11	0.23	−0.60	−0.19			−0.57	−0.65	−0.27	1.52	0.43	−0.62	−0.30	0.62	0.00	−0.06	0.67	0.94		
h			0.04	0.37	**−1.71**	−0.26			−0.38	−0.02	−0.40	1.29	0.26	−1.97	0.18	0.63	−0.13	−0.75	n.d.	n.d.		
i			0.34	0.71	−0.91	0.19			−0.77	−0.47	−0.23	2.06	n.d.	n.d.	−0.63	0.31	**0.04**	−1.28	0.94	0.84		
j			**0.37**	0.56	−1.00	−0.17			−0.65	−0.04			**0.78**	1.19	−0.79	0.40	−0.39	**−1.48**	1.42	1.28		
k			0.35	0.66	−2.07	−0.39							n.d.	n.d.	−0.45	0.17	−0.14	−1.17	1.25	0.83		
l			0.16	**0.77**	−1.09	0.01							**−0.32**	−2.89	−0.80	**−0.24**			0.76	0.54		
m			0.23	0.16	−0.69	0.12							−0.15	−2.69	−0.30	0.84			0.59	0.45		
n			−0.27	−0.02	−0.94	−0.30							−0.25	−3.01	−0.36	0.46			0.54	0.39		
o			−0.19	−0.18	−0.82	−0.93							−0.05	**−3.13**	−0.66	0.63			0.54	**0.07**		
p			−0.30	0.00	−0.43	0.04							−0.01	−3.10					0.56	0.12		
q			**−0.56**	−0.51	−1.51	**−2.02**							−0.01	−2.38					0.77	0.17		
r			−0.56	−0.44	−1.48	−1.12							n.d.	n.d.					n.d.	n.d.		
s			−0.27	−0.49	n.d.	n.d.							n.d.	n.d.					1.09	0.71		
t			−0.26	−0.41															1.40	0.84		
u			−0.14	−0.61															0.71	0.59		
v			−0.32	−0.41															0.59	0.42		
w			−0.39	**−0.69**															0.76	0.87		
x																			0.94	0.97		
y																			0.82	**1.37**		

Sub-sample [a] represents the latest shell part, respectively. Shells from 10, 30, 61 and 101 cm core depths were isotopically measured as bulk samples. Maxima and minima values are marked in bold

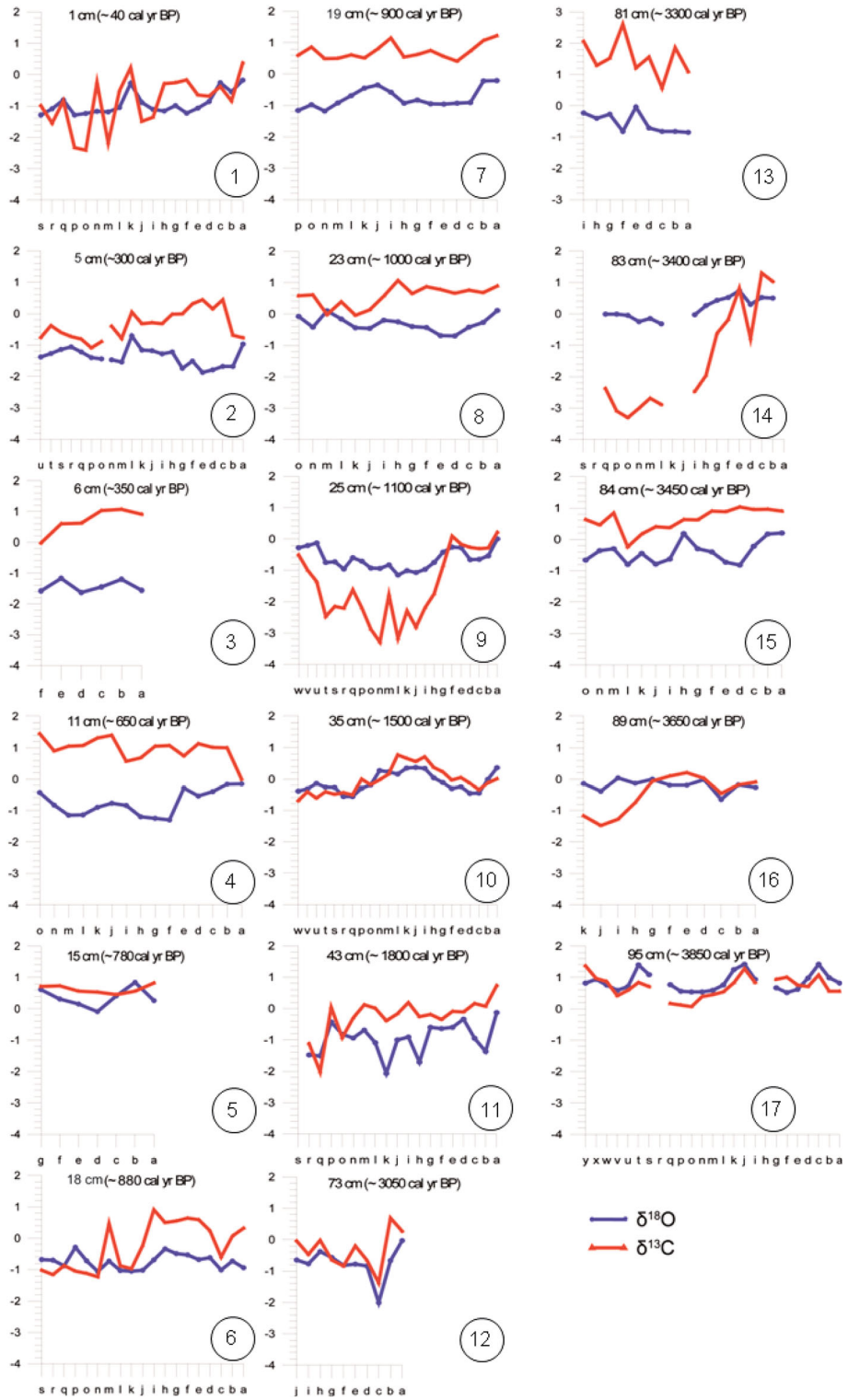

Fig. 4 Sclerochronological $\delta^{18}O$ and $\delta^{13}C$ patterns of all *Radix* shells. The letter 'a' represents the ontogenetically latest shell part

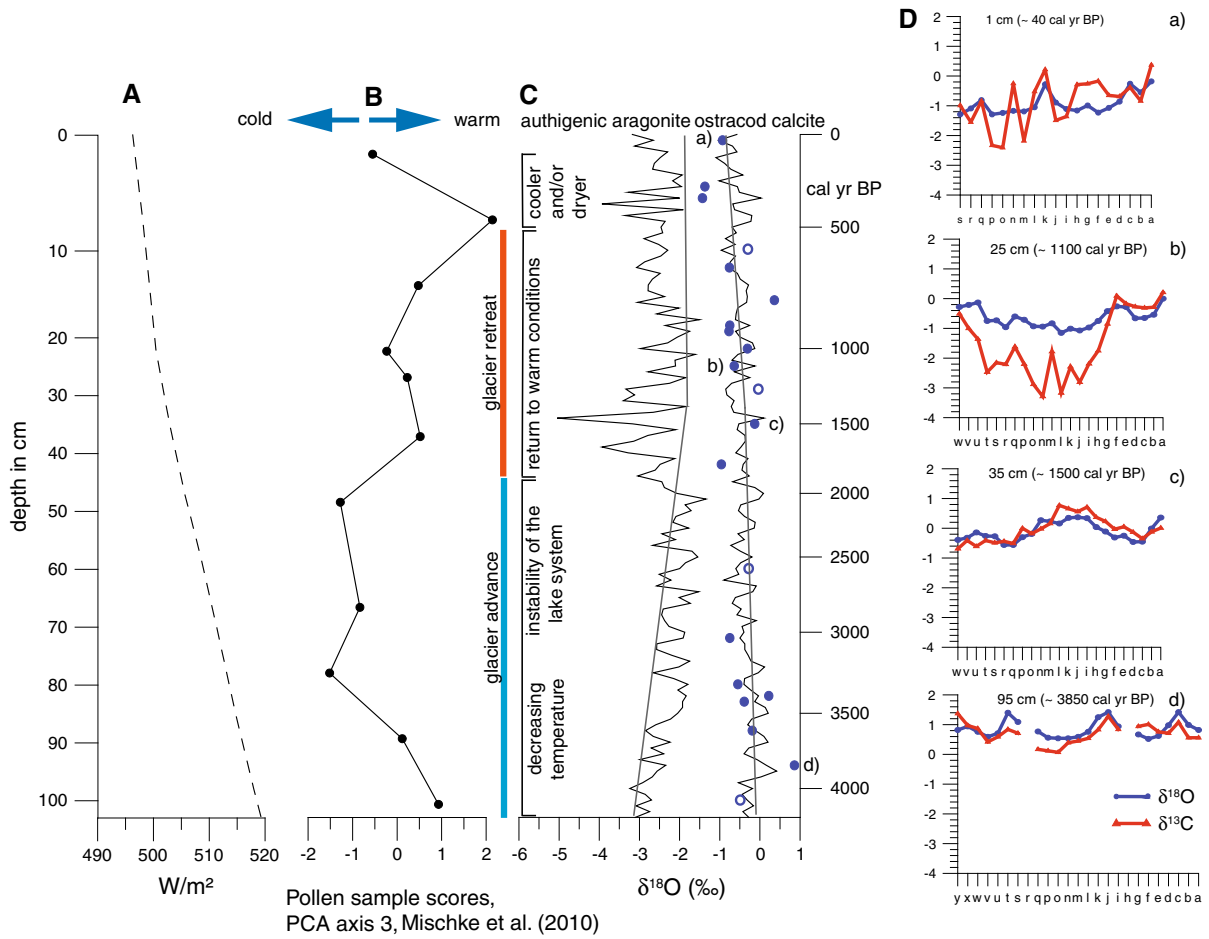

Fig. 5 **a** Summer (JJA) insolation curve for 39°N from 4,200 cal yr BP until present generated following Laskar et al. 2004). **b** Palynological data from the sediment core of Lake Karakul from Mischke et al. (2010). The sample scores of pollen principle component analysis (PCA) axis 3 mainly indicate air temperatures. **c** Mean $\delta^{18}O$ values from *Radix* shells (*filled blue circles*) in comparison to ostracod calcite, which represents the same habitat conditions, and authigenic aragonite, which represents surface water conditions. Four *Radix* shells were isotopically measured as bulk samples (*open blue circles*). The *gray lines* represent notional isotopic steady state conditions of the lake water. Lower-case letters illustrate the sections of the sclerochronological patterns representing the four different zones characterizing varying climate and environmental conditions at Lake Karakul (**d**). (Color figure online)

the similarity between the *Radix* shell data presented in this study and the ostracod isotope data is strong evidence that both shared the same habitat at the bottom of the shallow eastern basin of Lake Karakul. Differences, like the larger range of $\delta^{18}O$ values obtained for *Radix* samples compared with ostracod shells (Fig. 5c), might represent temporal differences in resolution and carbonate formation. One mean oxygen isotope value of a *Radix* shell averages about 1 year, whereas each ostracod sample represents ten individual shells, which may integrate the summer months of about 30 years (Mischke et al. 2010). The expected but not observed difference of +0.6 ‰ between isotope ratios of *Radix* aragonite and ostracod calcite might be due to vital effects (Grossman and Ku 1986; Abell and Williams 1989; Leng and Marshall 2004), or the fact that *Radix* shells represent a record of the lake water isotope composition over the whole year whereas ostracods solely form shells during the summer months. However, the similarity between the *Radix* and the ostracod shell isotope data demonstrates that the ostracod shells provide significant information

on the climatic and hydrologic history of Lake Karakul.

The $\delta^{18}O$ values of authigenic aragonite are on average ~2 ‰ lower and the range is significantly larger than what is recorded by ostracod shells (Mischke et al. 2010; Fig. 5c). Therefore it is impossible that the curves of authigenic aragonites and ostracod calcite shells mirror the same habitat. Authigenic carbonates in sediments are thought to form in the whole water column but will preferentially precipitate from warm, near surface waters during the summer months (Henderson et al. 2003; Liu et al. 2009). Therefore, authigenic aragonites hold primarily a record of the surface water of Lake Karakul during the summer. On average 2 ‰ lower $\delta^{18}O$ values can be explained by a ~8 °C temperature difference between surface and bottom water in Lake Karakul. The water temperature of the surface water during the summer months is around 11–13 °C (Mischke et al. 2010), and thus the bottom water would have a temperature of 3–5 °C, which seems to be reasonable. Facts about the lake stratification are unknown. However, the differences between the ostracod $\delta^{18}O$ curve on the one hand and the authigenic aragonite curve on the other hand indicate a generally stable stratification for Lake Karakul. Besides temperatures, the isotopic composition of the surface water might change faster than the bottom waters. Therefore, the surface waters from which authigenic aragonites precipitated are more sensitive to changes in the environment, melt water flux, or temperature than the bottom waters recorded in ostracod shells. This sensitivity or small residence time allows the record of short-term disturbances of the lake system, which can be used to divide the climatic and environmental evolution of Lake Karakul in distinct periods.

Late Holocene environmental evolution and climate conditions at Lake Karakul

The ostracod shell stable isotope data

The isotopic composition of ostracod shells exhibit a continuous development toward more negative $\delta^{18}O$ values in the past 4,200 cal yr BP (Mischke et al. 2010; Fig. 5c). The long-term trend is overlain by short-term excursions from a supposed isotopic steady state composition of the lake water. The short-term excursions in the ostracod dataset are thought to represent variations of the melt water fluxes to Lake Karakul over time scales of 20–40 years. The long-term trend reflects most likely a change in the isotopic compositions of the precipitation, which contributes to the glaciers as snow and finally as melt water to the lake. The shift towards lower $\delta^{18}O$ values of precipitations might be due to decreasing temperatures in the Karakul region. This is consistent with decreasing summer insolation at this latitude in the last 4,200 cal yr BP (Laskar et al. 2004; Fig. 5a). In addition, lower temperatures may correspond to higher relative air humidity over Lake Karakul and, thus a decreasing isotopic fractionation during evaporation of the lake water. Both shift the isotopic composition of the lake water towards more negative $\delta^{18}O$ values (Fig. 5c).

The authigenic aragonite stable isotope record

The authigenic aragonites recorded an increase of the $\delta^{18}O$ values of the surface water between 4,200 and 1,800 cal yr BP reflecting a larger isotope fractionation between carbonate and water due to decreasing average temperatures in the surface waters. The temperature effect explains why carbonates from surface waters and bottom waters exhibit discrepant trends in the Karakul sediment cores (Mischke et al. 2010, Fig. 5). At 1,800 cal yr BP the authigenic aragonites are shifted towards more negative $\delta^{18}O$ values, indicating strong warming of the surface water due to higher air temperatures. Furthermore, it is assumed that large masses of glacial melt water flowed into the lake during this period, which increased the trend to more negative oxygen isotope values. Possibly the continuous retreat of the glaciers have reached a tipping point where the albedo of the landscape has been reduced so much that temperatures in the summer months became warm enough to melt remaining glaciers at high altitudes. The melt water signal is recorded in the surface water of Lake Karakul but not as clear in the ostracod bottom water record because of the different sizes of the two reservoirs. Between 1,000 and 500 cal yr BP the temperature of the surface water decreased continuously and at about 350 cal yr BP the temperatures reached a minimum in the Karakul area probably representing an analogue to the cooling during the Maunder Minimum in the North Atlantic region. Subsequently the climate became warmer again indicated by low $\delta^{18}O$ values in the

authigenic aragonite curve. This climatic interpretation will be tested on an assessment of seasonal information from sclerochronological isotope patterns in *Radix* shells.

Seasonal changes during the Late Holocene at Lake Karakul

The sclerochronological stable isotope patterns of the fossil *Radix* shells can be used to test certain models on the nature of long-term variations seen in the authigenic aragonite and/or ostracod shell curves. For this purpose, we first distinguish between two different types of sclerochronological isotope patterns indicating (1) a meltwater signal, and (2) no meltwater signal. Taft et al. (2012, 2013) showed that rapidly decreasing $\delta^{18}O$ values and simultaneously decreasing $\delta^{13}C$ values result from glacial meltwater, which has low ^{18}O ratios and input of allochthonous carbon with low $\delta^{13}C$ values from the catchment and the upper soil layers. Shells 2, 4, 9, 11, 15 and 17 (Fig. 4) can be related to group (1) and shells 1, 6, 7, 8, 10, 14 and 16 (Fig. 4) can be related to group (2). Shells 3, 5, 12 and 13 (Fig. 4) do not cover a complete life cycle of the specimens and therefore do not show distinct seasonal patterns. We divided the isotope record in the Lake Karakul sediment core in three zones with varying influence of meltwater flux and air temperature.

Zone I (~4,200–1,800 cal yr BP, 104–45 cm core depth): Low lake level, increasing instability of the lake system, glacier advance, cooling

Information about the seasonal changes during this period is available for several *Radix* shells. *Radix* shell number 17 (Figs. 4, 5d) probably reflects slight meltwater input, indicated by decreasing $\delta^{18}O$ values from segment [t] to [m] and from [j] to [f], which is supported by slightly decreasing $\delta^{13}C$ values (Figs. 4, 5d). The more positive $\delta^{18}O$ and $\delta^{13}C$ values from [m] to [j] and from [f] to [c] in this shell mirror strong evaporation and biological activity in the lake, respectively. In general, the meltwater signal in this *Radix* shell is not well pronounced and the oxygen isotope values are positive during the whole life span of this specimen. Thus, at ~3,850 cal yr BP glacial meltwater input during the summer months is seen in the sclerochronological data but was likely relatively low. The sclerochronological stable isotope pattern of shell number 15 (~3,450 cal yr BP) shows a pronounced meltwater signal with more negative $\delta^{18}O$ values from sub-samples [h] to [d] (Fig. 4).

The overall gradual shift toward more negative $\delta^{18}O$ values in the ostracod data and increasing $\delta^{18}O$ values in the authigenic aragonite data indicates decreasing temperatures between 4,200 and 1,800 cal yr BP (Fig. 5) interrupted by a few short-term periods with enhanced meltwater input most likely due to an increase in precipitation and/or higher air temperatures. The $\delta^{18}O$ values of authigenic aragonite become more positive likely in response to a cooling of the surface lake water, which causes a stronger isotope fractionation between water and carbonate. The cooling during this period is connected with a reduction of the meltwater flux in several steps.

The authigenic carbonate curve shows that negative $\delta^{18}O$ excursions became more common towards the end of the period between 4,200–1,800 cal yr BP. Obviously, lake level fluctuated towards the end of this period. However, overall the *Radix* and authigenic carbonate data provide evidence for a decreasing melt water flux between 4,200 and 1,800 cal yr BP. It is assumed that the meltwater flux to the lake decreased mainly due to increasing precipitation in the glacial accumulation areas connected with a glacier advance. An abrupt shift to colder conditions around 3,500 cal yr BP is inferred from the TOC content as well as from the pollen composition by Mischke et al. (2010), but such a sharp shift is not recorded in the isotope data, most likely due to different sampling resolutions of these archives.

The interpretation of a glacier advance between 4,200–1,800 cal yr BP is in agreement with other proxy data from Asia. Remote sensing data, geomorphic mapping, and ^{10}Be terrestrial cosmogenic nuclide (TCN) surface-exposure dating of boulders (Seong et al. 2009) indicated advancing glaciers and cooling between 4.2 and 3.3 ka BP in the Muztag Ata and Kongur Shan region. Likewise, glaciers in the Ladakh and Zanskar Ranges of Transhimalaya advanced between 4.2 and 3.6 ka BP (Hedrick et al. 2011). A cold period was also inferred for other Central Asian records, e.g. from Bosten Lake in northwestern China from 3.4–3.2 ka cal yr BP (Wünnemann et al. 2006), the central Tienshan between 3.5–2.1 ka cal yr BP (Zhang et al. 2009) or the Guliya ice core on the northwestern Tibetan Plateau between 3.5–3.0 ka cal yr BP (Thompson et al. 2005).

Zone II (~1,800–500 cal yr BP, 44–8 cm core depth): Increasing meltwater input, increasing lake level, glacier retreat, warming

The sclerochronological pattern from *Radix* shell number 11 (~1,800 cal yr BP) indicates slight meltwater fluxes by low $\delta^{18}O$ and $\delta^{13}C$ values at sub-samples [l] and [b]. The pattern of *Radix* shell number 10 confirms the suggested change to warmer and probably drier conditions which caused a higher evaporation rate (Figs. 4, 5d) indicated by more positive oxygen isotope values. The carbon isotope pattern follows the oxygen isotope pattern, indicating equilibration of the TDIC with atmospheric CO_2 (Leng and Marshall 2004). However, the sclerochronological $\delta^{18}O$ pattern of *Radix* shell number 9 (~1,100 cal yr BP) shows a high meltwater flux represented by more negative values from sub-sample [u] to [i] and synchronously lower $\delta^{13}C$ values due to the input of isotopically light CO_2 from the catchment (Fig. 4). From sub-sample [j] to [a] the meltwater discharge decreases and more positive $\delta^{13}C$ values mirror probably both the increasing biological productivity in the lake and the reduced input of allochthonous carbon. More positive oxygen isotope values from [i] to [a] represent increasing evaporation. A more negative average $\delta^{18}O$ value of shell number 4 (~650 cal yr BP) indicates conditions relatively similar to shells 7 (~900 cal yr BP) and 6 (~880 cal yr BP; Fig. 4). However, the ^{18}O ratios of authigenic aragonite become more negative at the same time, which points to a change in the isotope water composition, possibly by increasing evaporation due to warmer conditions. The sclerochronological isotope pattern of shell 4 (Fig. 4) shows more positive $\delta^{18}O$ values from sub-samples [f] to [a] representing increasing evaporation. A slight meltwater signal is possibly shown from [i] to [f]. The $\delta^{13}C$ values are more positive and stable along the whole pattern indicating a high biological productivity in the lake which is supported by a relatively high TOC content (Mischke et al. 2010).

Mischke et al. (2010) also reconstructed a rather high freshwater inflow around 1,800–1,500 cal yr BP based on $\delta^{18}O$ values of authigenic aragonite. TOC values in the core increased as a result of higher lake productivity and palynological data indicate increasing temperatures and relatively wet conditions (Mischke et al. 2010; Fig. 5b). More negative $\delta^{18}O$ values of authigenic aragonite indicate warm surface water (Mischke et al. 2010; Fig. 5c).

Between ca. 1,800 and 1,500 cal yr BP, the $\delta^{18}O$ values of *Radix* shells, authigenic aragonite and ostracods point to a strong warming indicated by negative and positive excursions from the long-term trend for *Radix* shells, respectively (Fig. 5c). The whole period between 1,800–1,500 cal yr BP is characterized by a turnaround of the climate and environmental conditions at Lake Karakul, which was already foreshadowed by the previous period. Until ca. 1,800 cal yr BP, the glaciers in the catchment were thus far built up and the albedo was relatively high that a longer warm phase was needed to trigger an extensive glacier retreat. It is assumed that large masses of meltwater flowed into the lake and changed the isotope composition of the water, which is indicated by more negative $\delta^{18}O$ values of authigenic aragonite and ostracod calcite between ca. 1,400 and 1,200 cal yr BP (Mischke et al. 2010; Fig. 5c).

Subsequently, as a result of the glacier retreat, the albedo possibly decreased in this area. This self-reinforcing process most likely caused even warmer local conditions. These assumptions are primarily based on the core record from Mischke et al. (2010) due to the lack of sclerochronological data from the section between 1,400 and 1,200 cal yr BP. Between ca. 1,200 and 500 cal yr BP the lake system was characterized by fluctuations of warmer and slightly cooler conditions and varying lake levels, which is supported by the sclerochronological shell patterns. The mean $\delta^{18}O$ value of shell number 6 (~1,000 cal yr BP) is higher compared to shell number 7 (~900 cal yr BP) and is interpreted as a return to drier conditions which is supported by warmer surface water represented by negative $\delta^{18}O$ values of authigenic aragonite and a positive peak of $\delta^{18}O$ in the ostracod data set (Mischke et al. 2010; Fig. 5c).

Narama (2002) found evidence for a retreat of the large Raigorodskogo Glacier (Pamir-Altai) as a result of a warm period around 1,545 cal yr BP. In contrast, Seong et al. (2009) determined the age of moraines by ^{10}Be surface-exposure dating indicating a glacier advance around 1,400 cal yr BP in the Muztag Ata and Kongur Shan region in westernmost Tibet. Boomer et al. (2000) found evidence for a maximum regression phase of Lake Aral around 1,600 cal yr BP. The assumed strong warming around 1,500 cal yr BP

at Lake Karakul corresponded with the onset of the North Atlantic Medieval Warm Period and a maximum of the Indian monsoon intensity (Gupta et al. 2003).

Zone III (~500 cal yr BP-present, 8–0 cm core depth): Cool and dry (?) between ~500–300 cal yr BP, since ~300 cal yr BP increasing lake level and temperature?

The sclerochronological isotope pattern of shell 2 (Fig. 4) shows a meltwater signal from [l] to [e] by lower $\delta^{18}O$ values. However, the $\delta^{13}C$ values do not indicate a high flux of isotopically light carbon from the catchment into the lake, and instead, the values become more positive from [i] to [c]. Likely, the meltwater signal is overprinted by a temperature signal during the summer months and the $\delta^{13}C$ values indicate high biological productivity caused by higher temperatures and light intensity. The sclerochonological pattern of shell 1 (~40 cal yr BP) does not show a meltwater signal. This probably is due to slightly colder conditions compared to the previous section, and this is confirmed by more negative $\delta^{18}O$ ostracod values (Mischke et al. 2010; Fig. 5c). A high TOC content was recorded in the core, and palynological data indicate a tendency to slightly warmer and drier conditions around 400 cal yr BP (Mischke et al. 2010; Fig. 5b). Relatively cold and dry conditions are suggested for the period around 350 cal yr BP, which possibly represents an analogue for the cooling during the Maunder Minimum in Europe and the North Atlantic region (Mischke et al. 2010).

A slight warming is assumed for the period from ca. 300 cal yr BP until present. The reduced meltwater flux between 1,500 cal yr BP can be a result of lacking glacier masses in the catchment because it is assumed that they had melted to a large extent after this period after 1,500 cal yr BP. The slightly more positive $\delta^{18}O$ values of authigenic aragonite point to relatively cold surface water. However, the general trend to more negative values from ca. 300 cal yr BP until the present indicates increasingly warmer conditions.

This inference of recent warming corresponds to results of several studies that confirm negative glacier mass balances for Central Asia since the first half of the nineteenth century due to warmer conditions (Unger-Shayesteh et al. 2013). However, the ice volume of the glaciers in the catchment of Lake Karakul was relatively small after the previous melting period and the amount of the meltwater flux is assumed to be low.

The cooler and probably drier phase around 500 cal yr BP corresponds to inferred drier conditions from the Aral Sea between 500 and 400 cal yr BP (Boomer et al. 2000; Filippov and Riedel 2009) and from Sumxi Co (western Tibetan Plateau) at ca. 400 cal yr BP (Fontes et al. 1993). Parts of the Aral Sea catchment are located only about 200 km south of Lake Karakul.

Conclusions

Our results demonstrate that changes of the hydrologic system are not only triggered by meltwater fluxes on a short-time scale but are more complex and additionally controlled by changes in temperature and precipitation on a long time scale. The decreasing long term $\delta^{18}O$ trend of *Radix* and ostracod shells mainly indicates a change in the isotopic composition of precipitation which contributes to the glaciers in the catchment as snow and finally as melt water to the lake. The shift toward precipitation with low $\delta^{18}O$ values is likely related to decreasing temperatures in the Lake Karakul region. Over the last 4,200 years, the general isotopic composition of the lake water follows the decreasing solar insolation. This isotopic trend is overprinted by short-term meltwater fluxes. The similarity between the *Radix* and the ostracod $\delta^{18}O$ values suggests that both taxa lived in the same habitat. Furthermore, the similarity demonstrates that palaeoecological conclusions can be inferred from the studied ostracod taxon that Mischke et al. (2010) interpreted in a qualified manner.

The period between 4,200–3,000 cal yr BP is characterized by cooling, gradually decreasing lake level and, most likely, a glacier advance in the catchment. From ca. 3,000–1,800 cal yr BP, the lake system became instable but lake level remained low. During the following 600 years, glaciers retreated and lake level rose in response to warmer conditions and higher meltwater fluxes. The assumed strong warming around 1,500 cal yr BP probably represents the onset of the Medieval Warm Period. Warmer conditions and a higher lake level are indicated for the period until ca. 500 cal yr BP. A short relatively cold and probably dry period associated with a decreasing lake level is

assumed for the phase from around 350 cal yr BP, corresponding to an analogue of the cooling during the Maunder Minimum in the North Atlantic region. Subsequently, temperatures and lake level increased towards modern times.

Studying the isotopic composition of fossil *Radix* shells from Lake Karakul provided valuable additional information about the lake history for the last 4,200 cal yr BP. The sclerochronological isotope patterns in the shells helped to improve our knowledge about changes in seasonality. However, further studies are required to quantify the amount of former meltwater discharge, associated lake-level changes, and to investigate the glacial history in the catchment area.

Acknowledgments We are grateful to Maike Glos and Matthias Friebel (both FU Berlin) for the sample processing and to Nailya Mustaeva for logistical support during the fieldwork. Funding was provided by the Research Commission of the FUB, the Center for International Cooperation (FUB), the German Academic Exchange Service (DAAD) and the German Science Foundation (DFG). The comments of T.J. Whitmore and two anonymous reviewers greatly improved the manuscript.

References

Abell PI, Williams MAJ (1989) Oxygen and carbon isotope ratios in gastropod shells as indicators of paleoenvironments in the Afar Region of Ethiopia. Palaeogeogr Palaeoclimatol Palaeoecol 74:265–278

Bolch T (2007) Climate change and glacier retreat in northern Tien Shan (Kazakhstan/Kyrgyzstan) using remote sensing data. Glob Planet Change 56:1–12

Boomer I, Aladin N, Plotnikov I, Whatley R (2000) The palaeolimnology of the Aral sea: a review. Quat Sci Rev 19:1259–1278

ESRI (2011) ArcGIS desktop: release 10. Environmental Systems Research Institute, Redlands

Filippov A, Riedel F (2009) The late Holocene mollusk fauna of the Aral Sea and its biogeographical and ecological interpretation. Limnologica 39:67–85

Fontes JCh, Mélières F, Gibert E, Liu Q, Gasse F (1993) Stable isotope and radiocarbon balances of two Tibetan lakes (Sumxi Co, Longmu Co) from 13,000 BP. Quat Sci Rev 12:875–887

Goehring BM, Vacco DA, Alley RB, Schaefer JM (2012) Holocene dynamics of the Rhone Glacier, Switzerland, deduced from ice flow models and cosmogenic nuclides. Earth Planet Sci Lett 351–352:27–35

Gopal B, Ghosh D (2010) Lakes and reservoirs of Asia. Encyclopedia of inland waters, lake ecosystem ecology. In: Likens GE (ed) Academic Press, New York

Grossman EL, Ku TL (1986) Oxygen and carbon fractionation in biogenic aragonite: temperature effects. Chem Geol 59:59–74

Gupta AK, Anderson DM, Overpeck JT (2003) Abrupt changes in the Asian southwest monsoon during the Holocene and their links to the North Atlantic Ocean. Nature 421:354–356

Gurov EP, Gurova HP, Rakitskaya RB, Yamnichenko AY (1993) The Karakul depression in Pamirs: the first impact structure in Central Asia. Abstract Volume of the 24th Lunar and planetary science conference, Lunar and Planetary Institute, Lyndon B. Johnson Space Center Houston, pp 591–592

Hammer UT (1986) Saline lake ecosystems of the world. Monographiae Biologicae 59. Kluwer Academic Publication, Dordrecht

Hedrick KA, Seong YB, Owen LA, Caffee MW, Dietsch C (2011) Towards defining the transition in style and timing of Quaternary glaciations between the monsoon-influenced Greater Himalaya and the semi-arid Transhimalaya of Northern India. Quat Int 236:21–33

Henderson ACG, Holmes JA, Zhang J, Leng MJ, Carvalho LR (2003) A carbon- and oxygen-isotope record of recent environmental change from Qinghai Lake, NE Tibetan Plateau. Chin Sci Bull 48:1463–1468

Intergovernmental Panel on Climate Change IPCC (2007) Contribution of working group I to the fourth assessment report of the intergovernmental panel on climate change. In: Solomon SD, Qin M, Manning Z, Chen M, Marquis KB, Averyt M, Tignor MMB, Miller HL (eds) Cambridge University Press, Cambridge

Khromova TE, Osipova GB, Tsvetkov DG, Dyurgerov MB, Barry RG (2006) Changes in glacier extent in the eastern Pamir, Central Asia, determined from historical data and ASTA imagery. Remote Sens Environ 102:24–32

Komatsu T (2009) Field photographs of geomorphic features in the lake Karakul region, eastern Pamirs. Geogr Stud 84:44–50

Komatsu T, Watanabe T, Hirakawa K (2010) A framework for late Quaternary lake-level fluctuations in lake Karakul, eastern Pamir, focusing on lake–glacier landform interaction. Geomorphology 119:198–211

Kutuzov S, Shahgedanova M (2009) Glacier retreat and climatic variability in the eastern Terskey-Alatoo, inner Tien Shan between the middle of the 19th century and beginning of the 21st century. Glob Planet Change 69:59–70

Laskar J, Robutel P, Joutel F, Gastineau M, Correia ACM, Levrard B (2004) A long term numerical solution for the insolation quantities of the Earth. Astron Astrophys 428: 261–285, online data file http://www.imcce.fr/Equipes/ASD/insola/earth/online/index.php

Lehner B, Döll P (2004) Development and validation of a global database of lakes, reservoirs and wetlands. J Hydrol 296:1–22

Lehner B, Verdin K, Jarvis A (2006) HydroSHEDS technical documentation. World Wildlife Fund US, Washington, DC. http://hydrosheds.cr.usgs.gov

Leng MJ, Marshall JD (2004) Palaeoclimate interpretation of stable isotope data from lake sediment archives. Quat Sci Rev 23:811–831

Liu WG, Li XZ, Zhang L, An ZS, Xu LM (2009) Evaluation of oxygen isotopes in carbonate as an indicator of lake evolution in arid areas: the modern Qinghai Lake, Qinghai-Tibet Plateau. Chem Geol 268:126–136

Melack JM (1983) Large, deep salt lakes: a comparative limnological analysis. Hydrobiologia 105:223–230

Mischke S, Zhang CJ (2010) Holocene cold events on the Tibetan Plateau. Glob Planet Change 72:155–163

Mischke S, Rajabov I, Mustaeva N, Zhang C, Herzschuh U, Boomer I, Brown E, Andersen N, Myrbo A, Ito E, Schudack ME (2010) Modern hydrology and late Holocene history of Lake Karakul, eastern Pamirs (Tajikistan): a reconnaissance study. Palaeogeogr Palaeoclimatol Palaeoecol 289:10–24

Molchanov LA (1929) Lakes of Central Asia. Trudy Srednеaziat. Gos. Univ., Geografiya 3, pp. 26–31. Tashkent. (in Russian)

Narama C (2002) Late Holocene variation of the Raigorodskogo Glacier and climate change in the Pamir-Altai, central Asia. Catena 48:21–37

Narama C, Kääb A, Duishonakunov M, Abdrakhmatov K (2010) Spatial variability of recent glacier area changes in the Tien Shan Mountains, Central Asia, using Corona (~1970), Landsat (~2000), and ALOS (~2007) satellite data. Glob Planet Change 71:42–54

Ni A, Nurtayev B, Petrov M, Tikhanovskaya A, Tomashevskaya I (2004) The share of glacial feeding in water balance of Aral Sea and Karakul Lake. J Marine Syst 47:143–146

Osipov EY, Khlystov OM (2010) Glaciers and meltwater flux to Lake Baikal during the Last Glacial Maximum. Palaeogeogr Palaeoclimatol Palaeoecol 294:4–15

Owen LA, Kamp U, Spencer JQ, Haserodt K (2002) Timing and style of Late Quaternary glaciation in the eastern Hindu Kush, Chitral, northern Pakistan: a review and revision of the glacial chronology based on new optically stimulated luminescence dating. Quat Int 97–98:41–55

Peel MC, Finlayson BL, McMahon TA (2007) Updated world map of the Köppen-Geiger climate classification. Hydrol Earth Syst Sci 11:1633–1644

Ricketts RD, Johnson TC, Brown ET, Rasmussen KA, Romanovsky VV (2001) The Holocene paleolimnology of Lake Issyk-Kul, Kyrgyzstan: trace element and stable isotope composition of ostracods. Palaeogeogr Palaeoclimatol Palaeoecol 176:207–227

Safarov NM (2006) Republic of Tajikistan. National Environmental Action Plan. www.unpei.org/PDF/National_Environmental_Action_Plan_eng.pdf

Sarikaya MA, Zreda M, Çiner A (2009) Glaciations and paleoclimate of Mount Erciyes, central Turkey, since the Last Glacial Maximum, inferred from ^{36}Cl cosmogenic dating and glacier modeling. Quat Sci Rev 28:2326–2341

Scherler D, Bookhagen B, Strecker MR (2011) Spatially variable response of Himalayan glaciers to climate change affected by debris cover. Nat Geosci 4:156–159. doi:10.1038/ngeo1068

Seong YB, Owen LA, Bishop MP, Bush A, Clendon P, Copland L, Finkel R, Kamp U, Shroder JF (2007) Quaternary glacial history of the Central Karakoram. Quat Sci Rev 26:3384–3405

Seong YB, Owen LA, Yi C, Finkel RC (2009) Quaternary glaciations of Muztag Ata and Kongur Shan: evidence for glacier response to rapid climate changes throughout the Late Glacial and Holocene in westernmost Tibet. Geol Soc Am Bull 121:348–365

Solomina O, Barry R, Bodnya M (2004) The retreat of Tien Shan glaciers (Kyrgyzstan) since the Little Ice Age estimated from aerial photographs, lichenometric and historical data. Geogr Ann 86:205–215

Sorrel P, Popescu SM, Head MJ, Suc JP, Klotz S, Oberhänsli H (2006) Hydrographic development of the Aral Sea during the last 2000 years based on a quantitative analysis of dinoflagellate cysts. Palaeogeogr Palaeoclimatol Palaeoecol 234:304–327

Taft L, Wiechert U, Riedel F, Weynell M, Zhang HC (2012) Sub-seasonal oxygen and carbon isotope variations in shells of modern *Radix* sp. (Gastropoda) from the Tibetan Plateau: potential of a new archive for palaeoclimatic studies. Quat Sci Rev 34:44–56

Taft L, Wiechert U, Zhang HC, Lei GL, Mischke S, Plessen B, Weynell M, Winkler A, Riedel F (2013) Oxygen and carbon isotope patterns archived in shells of the aquatic gastropod *Radix*: hydrologic and climatic signals across the Tibetan Plateau in sub-monthly resolution. Quat Int 290–291:282–298

Thompson LG, Davis ME, Mosley-Thompson E, Lin P, Henderson KA, Mashiotta TA (2005) Tropical ice core records: evidence for asynchronous glaciation on Milankovitch timescales. J Quat Sci 20:723–733

Unger-Shayesteh K, Vorogushyn S, Farinotti D, Gafurov A, Duethmann D, Mandychey A, Merz B (2013) What do we know about past changes in the water cycle of Central Asian headwaters? A review. Glob Planet Change. doi: 10.1016/j.gloplacha.2013.02.004

Vasskog K, Paasche Ø, Nesje A, Boyle JF, Birks HJB (2012) A new approach for reconstructing glacier variability based on lake sediments recording input from more than one glacier. Quat Res 77:192–204

von Oheimb PV, Albrecht C, Riedel F, Du L, Yang JX, Aldridge DC, Bößneck U, Zhang HC, Wilke T (2011) Freshwater biogeography and limnological evolution of the Tibetan Plateau—Insights from a plateau-wide distributed gastropod taxon (*Radix* spp.). PLoS ONE 6:e26307. doi:10.1371/journal.pone.0026307

World Glacier Monitoring Service WGMS (2012) Global Glacier Changes: facts and figures. http://www.grid.unep.ch/glaciers/pdfs/glaciers.pdf

Wünnemann B, Mischke S, Chen FH (2006) A Holocene sedimentary record from Bosten Lake, China. Palaeogeogr Palaeoclimatol Palaeoecol 234:223–238

Zhang Y, Kong ZC, Yan S, Yang ZJ, Ni J (2009) "Medieval Warm Period" on the northern slope of central Tienshan Mountains, Xinjiang, NW China. Geophys Res Lett 36:L11702. doi:10.1029/2009GL037375